



Magnetic Coulomb Phase in the Spin Ice Ho2Ti2O7

T. Fennell, et al. Science **326**, 415 (2009); DOI: 10.1126/science.1177582

This copy is for your personal, non-commercial use only.

If you wish to distribute this article to others, you can order high-quality copies for your colleagues, clients, or customers by clicking here.

Permission to republish or repurpose articles or portions of articles can be obtained by following the guidelines here.

The following resources related to this article are available online at www.sciencemag.org (this information is current as of January 8, 2010):

Updated information and services, including high-resolution figures, can be found in the online version of this article at:

http://www.sciencemag.org/cgi/content/full/326/5951/415

Supporting Online Material can be found at:

http://www.sciencemag.org/cgi/content/full/1177582/DC1

A list of selected additional articles on the Science Web sites **related to this article** can be found at:

http://www.sciencemag.org/cgi/content/full/326/5951/415#related-content

This article **cites 25 articles**, 1 of which can be accessed for free: http://www.sciencemag.org/cgi/content/full/326/5951/415#otherarticles

This article has been **cited by** 1 articles hosted by HighWire Press; see: http://www.sciencemag.org/cgi/content/full/326/5951/415#otherarticles

This article appears in the following **subject collections**: Physics

http://www.sciencemag.org/cgi/collection/physics

Magnetic Coulomb Phase in the Spin Ice Ho₂Ti₂O₇

T. Fennell, ¹* P. P. Deen, ¹ A. R. Wildes, ¹ K. Schmalzl, ² D. Prabhakaran, ³ A. T. Boothroyd, ³ R. J. Aldus, ⁴ D. F. McMorrow, ⁴ S. T. Bramwell ⁴

Spin-ice materials are magnetic substances in which the spin directions map onto hydrogen positions in water ice. Their low-temperature magnetic state has been predicted to be a phase that obeys a Gauss' law and supports magnetic monopole excitations: in short, a Coulomb phase. We used polarized neutron scattering to show that the spin-ice material Ho₂Ti₂O₇ exhibits an almost perfect Coulomb phase. Our result proves the existence of such phases in magnetic materials and strongly supports the magnetic monopole theory of spin ice.

The spin ice family (1-3) is part of a larger class of magnetic materials that at low temperatures enter a thermodynamic state known as a cooperative paramagnet (4, 5). The spins are correlated, but competing interactions prevent long range order, so that the system fluctuates, exploring its many degenerate ground states. Typically, there is some local rule that can be used to construct these ground states. For example, in a spin ice ground states are obtained by ensuring that a "two spins in, two spins out" configuration is satisfied on every tetrahedron (Fig. 1A). Similar rules, generically termed "ice rules," control hydrogen atom positions in water ice (6), dimer configurations in spin liquids (7), and spin configurations in Heisenberg pyrochlore antiferromagnets (8). In theory, all these systems are effective Coulomb phases (9, 10) because the ice rule variables can be mapped to a nondivergent field, and excitations that break the constraint create effective monopoles (11, 12) in that field. The system obeys a Gauss' law, which relates divergences in a field to a pole density.

Theoretical work (10, 13) has recognized that the fundamental difference between a conventional paramagnet and a magnetic Coulomb phase is in the form of the spin correlation function at a large distance [see also (14) for the anal-

¹Institut Laue-Langevin, Grenoble 38042, France. ²Institut für

uous experimental signature for it. Thus, the pseudo-dipolar correlations in direct ("real") space Fourier transform into a set of pinchpoint singularities, resembling bow-ties, in the reciprocal space probed by a scattering experiment. Although pinch points have been predicted for various magnetic systems, they have only been clearly observed in the field-induced kagome ice phase of spin ice (15, 16). They appear to be absent in all candidate magnetic Coulomb phases (17-19), including the zero-field spin ice state (15, 20–23).

Previous unpolarized neutron scattering on spin ices, such as $Ho_2Ti_2O_7(1,3)$, has established that the dipolar spin ice model, in which the rareearth ions are coupled by the dipole-dipole interaction and competing superexchange, gives an accurate description of bulk and microscopic properties (20, 23). The underlying reason for the persistence of spin ice behavior in this more complex model is that the dipolar Hamiltonian

has been shown to have practically identical groundstates to the near-neighbor (ice rules) model (10, 24), a feature known as projective equivalence. The two differ by small corrections that are expected to vanish as r^{-5} . It is therefore strongly expected that the spin-spin correlations of Ho₂Ti₂O₇ should exhibit a pseudo-dipolar

The combination of both dipolar correlations and interactions is essential to the proposal that ice rule defects in Ho₂Ti₂O₇ and Dy₂Ti₂O₇ are genuine magnetic monopoles (11). A Gauss' law is obeyed by the magnetization M(r) and the magnetic H-field. Monopolar sources and sinks in M and H correspond to thermally excited spin flips (Fig. 1B) (11, 25). Although the Gauss' law is a consequence of the dipolar spin correlations, it is the physical dipolar interactions that cause the relevant fields to be the electrodynamic quantities M and H. The dipolar interactions are not in doubt, but the failure to resolve a pinch point in the zero-field spin ice state (15, 20-23) raises questions about the reality of the dipolar correlations and hence the theories built upon them: the accuracy of projective equivalence, the postulated magnetic Coulomb phase, and the existence of magnetic monopoles.

Neutron scattering estimates the scattering function $S^{\alpha\beta}(\mathbf{Q})$ in reciprocal space (here α , β = x, y, z), which is the required Fourier transform of the thermally averaged two-spin correlation function. Our polarized neutron experiments were configured to measure two independent components of the tensor $S^{\alpha\beta}(\mathbf{Q})$ that we label as spin flip (SF) and non-spin flip (NSF). Here, z is vertical and x(y) is defined to be parallel (perpendicular) to the scattering vector **Q** in the horizontal scattering plane. With vertical (or z)

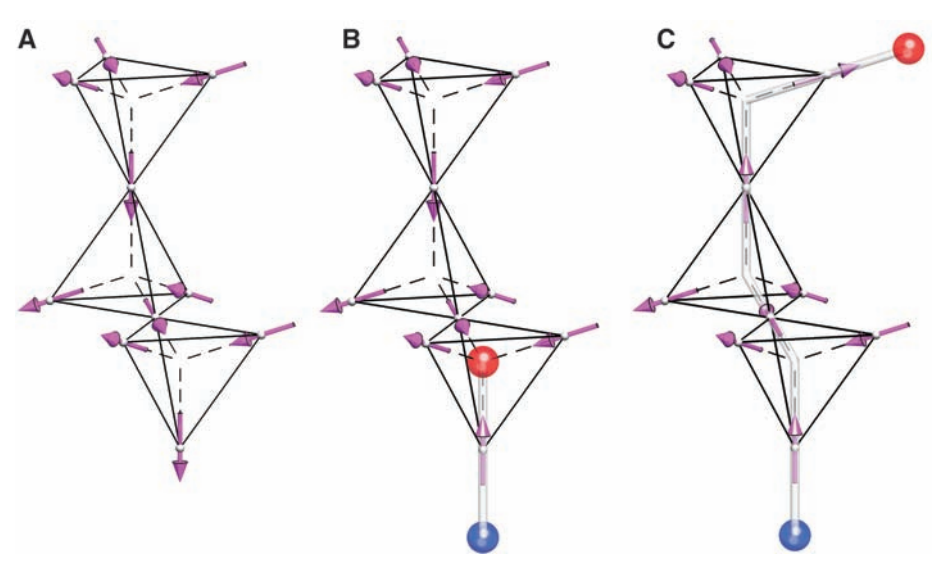


Fig. 1. Fragment of the spin ice structure. (A) The spin ice state in which each tetrahedron has the "two spins in, two spins out" configuration. (B) A single spin flip produces defects on two neighboring tetrahedra. (C) The defects can move apart. They interact like oppositely charged magnetic monopoles connected by a trail of flipped spins (a Dirac string). The pink arrows indicate spins, the blue spheres indicate monopoles, and the red spheres indicate antimonopoles.

ogous case of paraelectrics]. In the former, the spin correlation function decays like a screened Coulomb interaction; $\frac{1}{r} \exp^{-\kappa r}$, where κ is the inverse correlation length and r is the distance, whereas in the latter it is predicted to decay like a dipolar interaction $\sim \nabla_{\mathbf{r}} \nabla_{\mathbf{r}'} \frac{1}{\mathbf{r} - \mathbf{r}'}$. The dipolar form of the spin correlation function represents the Gauss's law (without poles) of the Coulomb phase and in principle affords an unambig-

Festkörperforschung, Forschungszentrum Juelich GmbH, Jülich Centre for Neutron Science at Institut Laue-Langevin, Grenoble 38042, France. ³Clarendon Laboratory, Oxford Physics, Parks Road, Oxford OX1 3PU, UK. 4London Centre for Nanotechnology and Department of Physics and Astronomy, University College London, London WC1H OAH, UK.

^{*}To whom correspondence should be addressed. E-mail: fennell@ill.fr

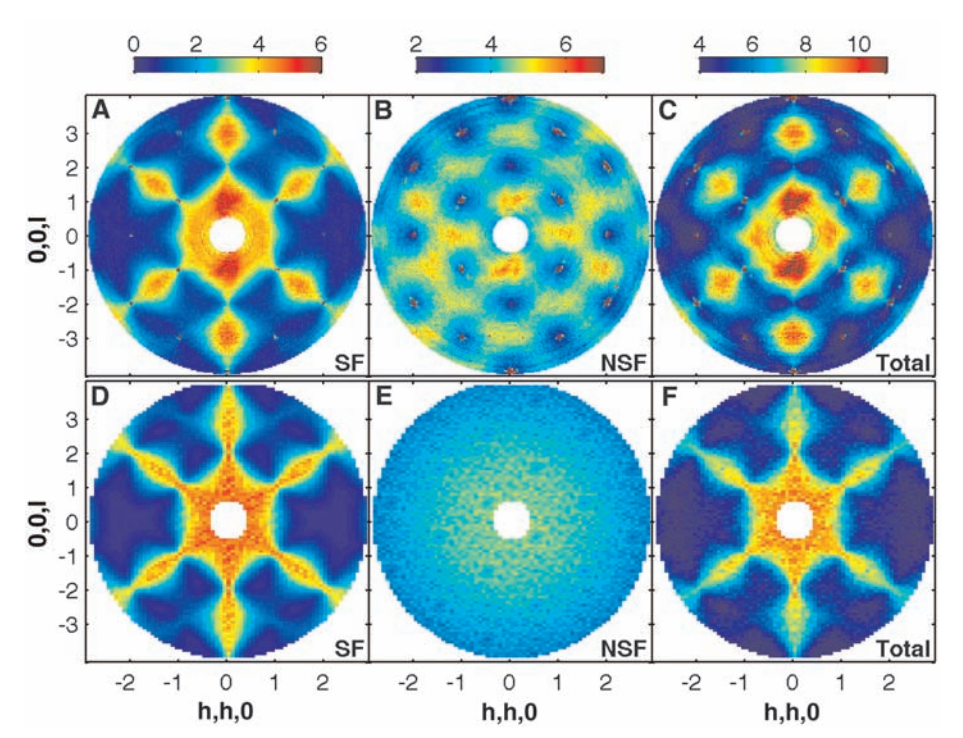


Fig. 2. Diffuse scattering maps from spin ice, $Ho_2Ti_2O_7$. Experiment [(**A**) to (**C**)] versus theory [(**D**) to (**F**)]. (A) Experimental SF scattering at T=1.7 K with pinch points at (0, 0, 2), (1, 1, 1), (2, 2, 2), and so on. (B) The NSF scattering. (C) The sum, as would be observed in an unpolarized experiment (20, 22). (D) The SF scattering obtained from Monte Carlo simulations of the near-neighbor model, scaled to match the experimental data. (E) The calculated NSF scattering. (F) The total scattering of the near-neighbor spin ice model.

incident neutron polarization, the SF and NSF cross sections yield information on $S^{yy}(\mathbf{Q})$ and $S^{zz}(\mathbf{Q})$, respectively. We used a single crystal of $\text{Ho}_2\text{Ti}_2\text{O}_7$ to map diffuse scattering in the h, h, l plane. Previous unpolarized experiments (20, 22) have measured the sum of the SF and NSF scattering, but in this orientation only the SF scattering would be expected to contain pinch points (26).

Our results (Fig. 2A) show that at temperature (T) = 1.7 K there are pinch points in the SF cross section at the Brillouin zone centres (0, 0, 2), (1, 1, 1), and (2, 2, 2) (Fig. 2A) but not in the NSF channel (Fig. 2B). The total scattering (SF + NSF) reveals the pinch points only very weakly (Fig. 2C) because the NSF component dominates near the zone center. This is explicitly illustrated with cuts across the zone center showing that the strong peak at the pinch point in the SF channel is only weakly visible in the total (Fig. 3B). The total scattering (Figs. 2C and 3B) can be compared with the previous observations and calculations (20, 22), in which no pinch points were detected. The use of polarized neutrons extracts the pinch-point scattering from the total scattering, and the previous difficulty in resolving the pinch point is clearly explained.

The projective equivalence of the dipolar and near-neighbor spin ice models (10) suggests that above a temperature scale set by the r^{-5} corrections, the scattering from Ho₂Ti₂O₇ should

become equivalent to that of the near-neighbor model. T = 1.7 K should be sufficient to test this prediction because it is close to the temperature of the peak in the electronic heat capacity that arises from the spin ice correlations [1.9 K (20)]. In our simulations of the near-neighbor spin ice model (Fig. 2, D to F), the experimental SF scattering (Fig. 2A) appears to be very well described by the near-neighbor model, whereas the NSF scattering is not reproduced by the theory. However, we have discovered that $S(\mathbf{Q})^{\text{experiment}}/S(\mathbf{Q})^{\text{theory}}$ is approximately the same function $f(\mathbf{O})$ for both channels. Thus, because the theoretical NSF scattering function is approximately constant, we find $f(\mathbf{Q}) \approx S(\mathbf{Q})_{\text{NSF}}^{\text{experiment}}$ This function may be described as reaching a maximum at the zone boundary and a finite minimum in the zone center. Using the above estimate of $f(\mathbf{Q})$, the comparison of the quantity $S(\mathbf{Q})_{\rm SF}^{\rm experiment}/f(\mathbf{Q})$ with $S(\mathbf{Q})_{\rm SF}^{\rm theory}$ is considerably more successful. Differences are less than 5% throughout most of the scattering map (26).

Cuts through the pinch point at (0, 0, 2) at 1.7 K (Fig. 3, A and B) show that it has the form of a low sharp saddle in the intensity. In order to better resolve the line shape of the pinch point, we performed an analogous polarized neutron experiment on a higher-resolution spectrometer. To compare with theory, we used an approximation to an analytic expression (13, 27).

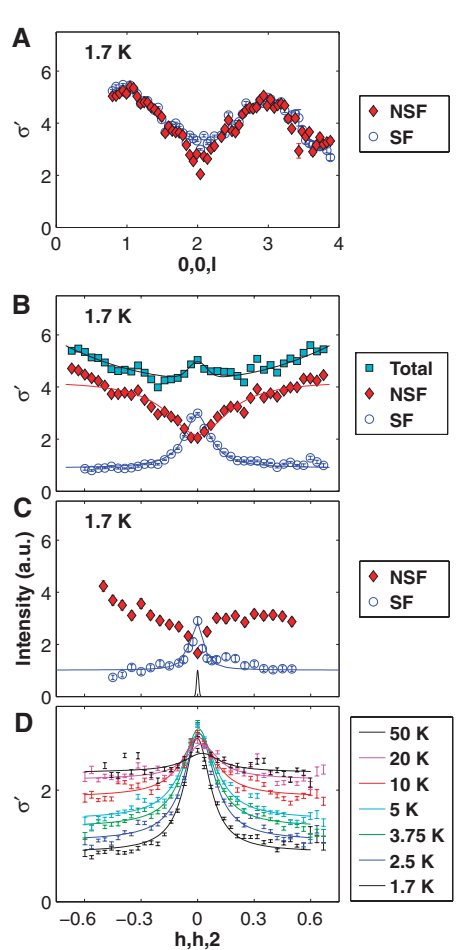


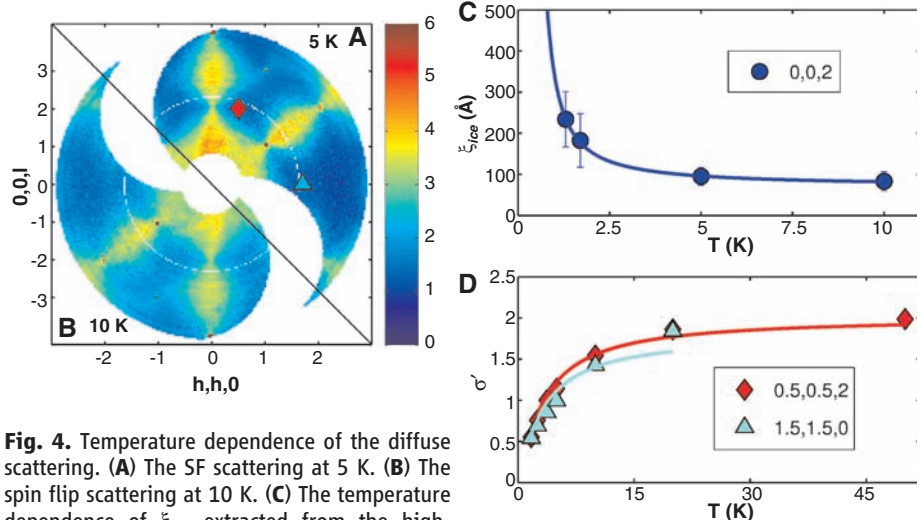
Fig. 3. Line shape of the pinch point. **(A)** Radial scan on D7 through the pinch point at (0, 0, 2) [of is the neutron scattering cross section; see (26) for its precise definition]. **(B)** The corresponding transverse scan. The lines are Lorentzian fits. **(C)** Higher-resolution data, in which the line is a resolution-corrected fit to the pinch point form Eq. 1 (the resolution width of the spectrometer is indicated as the central Gaussian). **(D)** SF scattering at increasing temperatures (the lines are Lorentzians on a background proportional to the Ho³⁺ form factor)

In the vicinity of the (0, 0, 2) pinch point, this becomes

$$S^{yy}(q_h, q_k, q_l) \propto \frac{q_{l-2}^2 + \xi_{\text{ice}}^{-2}}{q_{l-2}^2 + q_h^2 + q_k^2 + \xi_{\text{ice}}^{-2}}$$
(1)

Here, $\xi_{\rm ice}$ is a correlation length for the ice rules that removes the singularity at the pinch point (27). The high-resolution data of Fig. 3C can be described by this form, with a correlation length $\xi_{\rm ice} \approx 182 \pm 65$ Å, representing a correlation volume of about 14,000 spin tetrahedra. The correlation length has a temperature variation that is consistent with an essential singularity $\sim \exp(B/T)$, with $B = 1.7 \pm 0.1$ K (Fig. 4C).

The scattering in the NSF channel is concentrated around Brillouin zone boundaries, as



scattering. (A) The SF scattering at 5 K. (B) The spin flip scattering at 10 K. (C) The temperature dependence of ξ_{ice} extracted from the high-

resolution data fitted to an exponential divergence in T^{-1} . (**D**) Temperature dependence of the cross section σ' at (0.5, 0.5, 2) (the pinch-point background in Fig. 3D) and (1.5, 1.5, 0) [indicated by corresponding symbols in (A)]. The lines are fits to Eq. 2 (there is a fitted scale factor).

previously observed in unpolarized cross sections for both Ho₂Ti₂O₇ (22) and Dy₂Ti₂O₇ (21, 23). The NSF scattering shows a pronounced symmetric minimum at each Brillouin zone center, which is roughly as sharp as the maximum in the SF scattering (Fig. 3C). The sharp but finite minimum indicates an effect that tends to suppress long-range spin correlations but fails to do so completely: The pinch point and associated dipolar correlations remain. The distinct structure of the NSF scattering (which persists to temperatures as high as 10 K) suggests a simple and generic correction to the near-neighbor model emerging from the dipolar interaction. The lowtemperature evolution of the zone boundary scattering suggests that it is linked to corrections that become more important at low temperatures (22).

The general effect of increasing temperature on the SF scattering pattern (Fig. 4A) shows that empty areas of S^{yy} (for example, near 1.5, 1.5, 0) are increasingly filled in as the temperature rises, with a thermal contribution that is independent of wave vector (apart from the Ho³⁺ form factor), indicating uncorrelated point defects. We identify these as monopoles that remain strongly bound as dipole pairs (Fig. 1B). This behavior is also illustrated in Fig. 3D, in which, with increasing temperature, there is a marked decrease in peak intensity and an increase in the background on which the peak stands. As shown in Fig. 4D, this contribution can be generally fitted by the form

$$I(T) \simeq \frac{\exp(-2J/T) + \exp(-8J/T)}{1 + \exp(-2J/T) + \exp(-8J/T)}$$
 (2)

where I(T) is the intensity and $J \equiv J_{\text{eff}} = 1.8 \text{ K}$, which is the effective, near-neighbor exchange that is appropriate for Ho₂Ti₂O₇ (3). The two terms in the numerator are the cost of creating "singly charged" (monopole) or "doubly charged" thermal defects in the ice rules, respectively.

Two monopoles created by a spin flip can diffuse apart, leaving a path of successive headto-tail spins, which is known as a Dirac string (Fig. 1C) by analogy with Dirac's theory of magnetic monopoles. In spin ice, the strings carry local magnetization. If strings exist with lengths up to $\sim \xi_{ice}$, then this should be manifested as an approximately Lorentzian scattering with width ξ_{ice}^{-1} . Hence, we can attribute the broadening of the pinch point to the existence of unbound defects connected by Dirac strings with lengths up to ξ_{ice} (11, 25). At high temperatures, the proliferation of bound defects will both disrupt existing strings and reduce the mean free path for diffusing monopoles, reducing the maximum length in the Dirac string network. As the temperature is reduced, the thermal defect population decreases, and ξ_{ice} diverges as approximately $\exp(B/T)$ (Fig. 4C), with the observed value of B close to the effective exchange $J_{\text{eff}} = 1.8 \text{ K}$ (3). Such a temperature variation of ξ_{ice} is the same as that of the correlation length of the onedimensional Ising ferromagnet, which is indeed the maximum length of a ferromagnetic string in that system.

Investigation of the spin ice Ho₂Ti₂O₇ by use of polarized neutron scattering has established the validity of projective equivalence (24) and quantified the corrections to it. We have established that Ho₂Ti₂O₇ exhibits an almost ideal magnetic Coulomb phase, the quasiparticle vacuum for magnetic monopoles (11, 25). We have shown that bound monopole pairs dominate at finite temperature, but that unbound pairs become relatively more important at low temperatures. The length of the longest Dirac

strings has been estimated to rise to macroscopic scales as the temperature passes below 1 K.

References and Notes

- 1. M. J. Harris, S. T. Bramwell, D. F. McMorrow, T. Zeiske, K. W. Godfrey, Phys. Rev. Lett. 79, 2554 (1997).
- 2. A. P. Ramirez, A. Hayashi, R. J. Cava, R. Siddharthan, B. S. Shastry, Nature 399, 333 (1999).
- 3. S. T. Bramwell, M. J. P. Gingras, Science 294, 1495
- 4. J. Villain, Z. Phys. B 33, 31 (1979).
- 5. H. T. Diep, Frustrated Spin Systems (World Scientific, Singapore, 2004).
- 6. L. Pauling, J. Am. Chem. Soc. 57, 2680 (1935).
- 7. D. A. Huse, W. Krauth, R. Moessner, S. L. Sondhi, Phys. Rev. Lett. 91, 167004 (2003).
- 8. R. Moessner, J. T. Chalker, Phys. Rev. B 58, 12049
- 9. F. Alet, G. Misguich, V. Pasquier, R. Moessner, J. L. Jacobsen, Phys. Rev. Lett. 97, 030403 (2006).
- 10. S. V. Isakov, K. Gregor, R. Moessner, S. L. Sondhi, Phys. Rev. Lett. 93, 167204 (2004).
- 11. C. Castelnovo, R. Moessner, S. L. Sondhi, Nature 451, 42 (2008)
- 12. M. Hermele, M. P. A. Fisher, L. Balents, Phys. Rev. B 69, 064404 (2004).
- 13. C. L. Henley, Phys. Rev. B 71, 014424 (2005).
- 14. R. W. Youngblood, J. D. Axe, B. M. McCoy, Phys. Rev. B 21, 5212 (1980).
- 15. T. Fennell, S. T. Bramwell, D. F. McMorrow, P. Manuel, A. R. Wildes, Nat. Phys. 3, 566 (2007).
- 16. Y. Tabata et al., Phys. Rev. Lett. 97, 257205 (2006).
- 17. R. Ballou, E. Leliévre-Berna, B. Fåk, Phys. Rev. Lett. 76, 2125 (1996).
- 18. S.-H. Lee et al., Nature 418, 856 (2002).
- 19. K. Tomiyasu et al., Phys. Rev. Lett. 101, 177401
- 20. S. T. Bramwell et al., Phys. Rev. Lett. 87, 047205
- 21. T. Fennell et al., Phys. Rev. B 70, 134408 (2004).
- 22. J. P. Clancy et al., Phys. Rev. B 79, 014408
- 23. T. Yavors'kii, T. Fennell, M. J. P. Gingras, S. T. Bramwell, Phys. Rev. Lett. 101, 037204 (2008).
- 24. S. V. Isakov, R. Moessner, S. L. Sondhi, Phys. Rev. Lett. 95. 217201 (2005).
- 25. L. D. C. Jaubert, P. C. W. Holdsworth, Nat. Phys. 5, 258 (2009).
- 26. Supporting online material is available on Science Online
- 27. R. W. Youngblood, J. D. Axe, Phys. Rev. B 23, 232 (1981).
- 28. We thank P. Holdsworth, L. Jaubert, S. Calder, M. Harris, J. Chalker, C. Castelnovo, A. Fisher, L.-P. Regnault, and R. Moessner for valuable discussions and L. Fodinger, J. Previtali, O. Losserand, and A. Filhol for technical assistance with D7. IN12, cryogenics, and computation, respectively. We acknowledge the Engineering and Physical Sciences Research Council, Science and Technology Facilities Council, and Royal Society for funding.

Supporting Online Material

www.sciencemag.org/cgi/content/full/1177582/DC1 SOM Text Figs. S1 and S2 References

11 June 2009; accepted 26 August 2009 Published online 3 September 2009: 10.1126/science.1177582 Include this information when citing this paper.